THE JOURNAL OF BIOLOGICAL CHEMISTRY
Vol. 279, No. 19, Issue of May 7, pp. 20422–20434, 2004

Cardiac Overexpression of Myotrophin Triggers Myocardial Hypertrophy and Heart Failure in Transgenic Mice*Ⓢ

Received for publication, August 1, 2003, and in revised form, January 25, 2004
Published, JBC Papers in Press, February 16, 2004, DOI 10.1074/jbc.M308488200

Sagartirtha Sarkar, Douglas W. Leaman‡, Sudhiranjan Gupta, Parames Sil, David Young,

WITHDRAWN
October 7, 2020

This article has been withdrawn by Sagartirtha Sarkar, Douglas W. Leaman, Parames Sil, Annitta Morehead, Debabrata Mukherjee, Joe Hollyfield, and Subha Sen. Sudhiranjan Gupta, David Young, Norman Ratliff, Yaping Sun, and Mary Rayborn could not be reached. The images from 1-year-old mice shown in Fig. 1*A* were reused in the subsequent JBC article Sarkar, S., *et al.* (2004) *J. Biol. Chem.* **279,** 52630–52642 as 9-month-old mice. The images shown in Fig. 1*C* (*II*) as 18-week-old mice were also reused in the same publication (Sarkar, S., *et al.* (2004) *J. Biol. Chem.* **279,** 52630–52642) as 9-month-old mice. The GAPDH immunoblot shown in Fig. 2*B* (*1*) was reused in Sarkar, S., *et al.* (2004) *J. Biol. Chem.* **279,** 52630–52642. The withdrawing authors do not agree to the Journal's decision as the concerned images of Fig. 1 were reused in the second JBC article (Sarkar, S., *et al.* (2004) *J. Biol. Chem.* **279,** 52630–52642) only to introduce the model in that article as per the reviewer's suggestion, and no new data were put forward using these image panels. The withdrawing authors also disagree with the Journal's statement of the reuse of the GAPDH immunoblot. The withdrawing authors requested the journal to not withdraw this publication because no data in this particular article are in question and the subsequent JBC article (Sarkar, S., *et al.* (2004) *J. Biol. Chem.* **279,** 52630–52642) is to be withdrawn by the authors for the same figure panel duplication. The request was however declined by the Journal. The withdrawing authors have pointed out that the above-referenced article was 17 years ago, and their original documents were not saved after 15 years. In the absence of original data and figures, the withdrawing authors were unable to meet the criteria for the Journal. The withdrawing authors stand by the results and conclusions of this article and state that no data in this particular article were compromised in any way.

article must therefore be hereby marked "*advertisement*" in accordance with 18 U.S.C. Section 1734 solely to indicate this fact.
Ⓢ The on-line version of this article (available at http://www.jbc.org) contains an additional table.

** To whom correspondence should be addressed: Dept. of Molecular Cardiology (NB 50), The Cleveland Clinic Foundation, 9500 Euclid Ave., Cleveland, Ohio 44195. Tel.: 216-444-2056; Fax: 216-444-3110; E-mail: sens@ccf.org.

[1] The abbreviations used are: MHC, major histocompatibility complex; ANF, atrial natriuretic factor; Tg, transgenic; myo, myotrophin; HW, heart weight; BW, body weight; WT, wild type; LV, left ventricular; TBS, Tris-buffered saline; SOM, self-organizing map; TNF, tumor necrosis factor; EST, expressed sequence tag; TGF, transforming growth factor.

EXPERIMENTAL PROCEDURES

Animals—Animal studies were approved by the institutional Animal Research Committee according to internal policies and guidelines of the National Institutes of Health for the humane care and use of animals in research.

Generation of Transgenic Mice—An α-MHC-myotrophin transgene was constructed using a recombinant myotrophin (myo) in pcDNA3-myo-vector. We designed a 72-base oligomer carrying the 5′ skeletal α-actin untranslated region and used it to generate a chimeric myo-cDNA, placed adjacent to the cytomegalovirus promoter of pcDNA3. The α-MHC promoter-containing vector was provided by Dr. Jeffrey Robbins (University of Cincinnati). This vector has an α-MHC promoter and a heterologous 3′-untranslated region containing the human growth hormone poly(A) site. The α-MHC-myo-recombinant vector was digested using the NotI restriction enzyme. The resulting linear DNA fragment containing the α-MHC promoter-myo coding sequence and human growth hormone poly(A) was isolated and purified using Qiagen gel extraction kit (Qiagen, Valencia, CA). Pronuclear injection was performed at the University of Cincinnati transgenic animal facility, using standard techniques.

Determination of the Ratio of Heart Weight to Body Weight—Mice were euthanized by CO_2 and autopsied immediately for gross signs of heart failure, inflammatory lesions, or congenital defects. The hearts were then removed, washed with 1× phosphate-buffered saline, blotted dry, and weighed in a Mettler precision balance (Mettler-Toledo, Inc., Columbus, OH). Hypertrophy was measured using the heart weight (HW)/body weight (BW) in mg/g (3).

Hybridization Analysis—Four founder mice were identified by Southern blot analysis of genomic DNA (10 μg) prepared from tail biopsies. Northern blots were performed with ~20 μg of total cardiac RNA. The labeled myotrophin cDNA probe was generated using random primers, as described previously (9).

Quantitation of Myotrophin Protein—Western blots were p
using 10 μg of total protein from 9-month-old wild-ty
transgenic (Tg) mice hearts via standard techniques
anti-myotrophin antibody and was normalized u
phosphate dehydrogenase antibody (Novus
CO). Myotrophin from the hearts of Tg a
described previously (8).

RNase Protection Assay—To
weeks and 9 months old;
(10), and 15 μg was used
specific for growth factors
er's protocol (RiboQuant; B
RNase digestion, protected f
polyacrylamide gels and quan
malized the value of each hy
control, glyceraldehyde-3-phosph

Determination of Cardiac Func
graphy was performed at the Imag
Clinic's Department of Cardiovascular Medicine. Lightly sedated Tg and WT mice (4- and 36-week-old), using 0.2 ml of Avertin (99% *tert*-amyl alcohol and 99% 2,2,2-tribromoethanol; Aldrich), were evaluated using the M-mode views on a transthoracic study, measuring left ventricular (LV) systolic and diastolic dimensions, interventricular septum and LV posterior wall thickness, and left atrial chamber diameter. End-diastolic and end-systolic frames were defined as those showing the largest and smallest areas, respectively. Data were correlated with timing of the QRS complex. Digitized images were obtained using an ultrasound system (Hewlett-Packard Sonos 5500; Palo Alto, CA).

Histology—All hearts were fixed, paraffin-embedded, and cut into 4-μm sections. Sections (taken from same areas of the heart of WT and Tg mice) were stained with hematoxylin/eosin for structural analysis using standard techniques, and myocyte dimensions were quantitated by image scanning using the Image Pro Plus software program.

Isolation of Cardiac Myocytes from Hearts of Adult FVB and Tg Mice Overexpressing Myotrophin (11)—Hearts were taken out from heparin-injected mice and were cannulated via aorta ($n = 6$). Hearts were perfused with perfusion buffer (glucose (1 g), $NaHCO_3$ (0.58 g), and pyruvic acid (0.27 g), pH 7.3) with 95% O_2 and 5% CO_2 on a Langendorff apparatus. After perfusing the heart for 10 min in EGTA-supplemented perfusion buffer, hearts were digested using collagenase (2 mg/ml) for 28 min, with gradual enhancement of $CaCl_2$. After 28 min of digestion with collagenase, the heart was taken out and incubated in a diluted collagenase solution for 10 min in a shaking water bath at 37 °C. The ventricles were separated from the atria, triturated for 30 s, and subsequently filtered through cheesecloth. The filtrate was centrifuged at 400 rpm for 2 min, the supernatant was removed, and the pellet was resuspended in 4% bovine serum albumin solution and observed under a phase-contrast microscope. Preparations with 80–85% beating rod-shaped cells were used for experimental purposes.

Immunocytochemical Staining Using myo Antibody (12)—The cells were plated on slides coated with laminin and were fixed in 4% paraformaldehyde dissolved in 1× TBS for 10 min. Cells were then permeabilized with 0.1% Triton X-100 in 1× TBS for 5 min. The cells were blocked with heat-inactivated 4% horse serum and 0.1% sodium azide for 2 h. Cells were incubated overnight with primary antibody (8) (polyclonal anti-myotrophin) at 4 °C, washed extensively with 0.1% Triton X-100 in 1× TBS, and incubated with fluorescein isothiocyanate-conjugated goat anti-rabbit IgG (Jackson ImmunoResearch Laboratories, Inc., West Grove, PA) for 2 h at room temperature in the dark. The slides were extensively washed with 0.1% Triton X-100 in 1× TBS and once with 1× TBS. The cells were mounted on coverslips with 4′,6-diamidino-2-phenylindole and were observed under a fluorescent microscope.

Statistical Analysis—Results were expressed as mean ± S.E. Data was analyzed by two-way analysis of variance, and differences between groups were determined by a least-square means test (SUPERNOVA). A value of $p < 0.05$ was consid
significant.

Gene Array Studies—Ge
analyses utilized RNA from heart tissue isolated from W
ged 4 weeks (initiation of hypertrophy) or 36 we
on from hypertrophy to heart failure). Five
n each age group were examined. Tot
se transcribed, and double-stra
to cRNA (Enzo Bioarray
, Santa Clara, CA). Bio-
ted into cRNA during
RNA was fragmented
murine genome U74Av2
sets (Affymetrix), and hybrid-
washed, stained with streptavidin-
a confocal microscope scanner with a

ta were analyzed using the Microarray Suite and
software packages (Affymetrix). Genes identified as
were consistently increased in each pairwise comparison
the animals of interest (such as 9-month-old Tg mice) and all
er animals of both age groups (p values varying from 0 to 0.0025). Up-regulated genes were screened to eliminate those with "marginal" or "absent" absolute calls in the induced samples. Genes marked as down-regulated were consistently decreased among all pairwise comparisons (p values ranging from 0.90 to 1). -Fold change was calculated by converting average signal log ratio values (change in the expression level of a transcript between the control and experimental samples) for each probe set to a whole number. This was accomplished by raising 2 to the power of the signal log ratio value ($2^{(\text{signal log ratio})}$).

Gene clusters with similar expression patterns were identified using the self-organizing map (SOM)-clustering algorithm (10) of the Data Mining Tool software package (version 3.0; Affymetrix). Signal values for all genes were imported from the Microarray Suite (version 5.0) into the Data Mining Tool after publication using MicroDB software (Affymetrix) (13). SOM clustering was performed using default filtering values and parameters set to identify up to 81 possible clusters. After clustering, results again were screened to eliminate genes that failed to attain a "present" call in any of the pertinent samples.

Detailed tables for the changes in gene expression between failing and nonfailing hearts are provided as Supplemental Material (Supplemental Table I).

RESULTS

Generation of Tg Mice

Four founders were identified from the live births resulting from pronuclear injection (42 mice) with the myotrophin transgene. All four lines were expanded by crossing with non-Tg mice. The transmission rate of α-MHC myotrophin transgenic mice showed a 45% transmission frequency, determined by Southern analysis, typical of a Mendelian inheritance (line 1, 81/156 (52%); line 2, 7/32 (22%); line 3, 20/51 (39%); line 4, 20/51 (39%)). The ventricles and atria were enlarged significantly in all four lines of Tg mice by 4 weeks of age compared

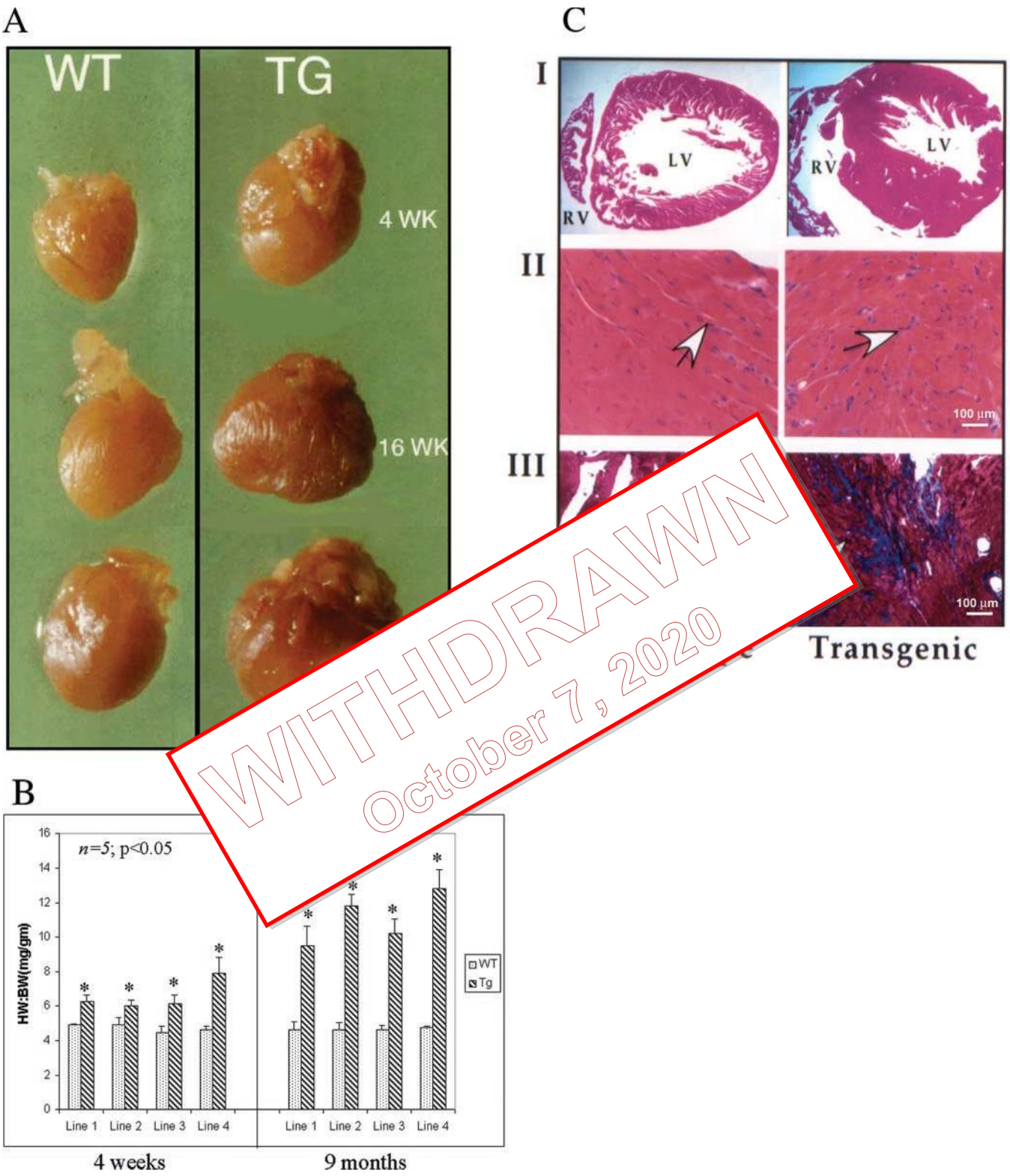

FIG. 1. *A*, hearts from the WT and Tg mice during progression of cardiac hypertrophy. *B*, quantitative estimation of HW/BW in all four lines of WT and Tg mice during initiation of hypertrophy (4 weeks old) and transition from hypertrophy to heart failure (9 months old). *C*, tissue histology and immunocytochemistry of 18-week-old wild-type (*left*) and 18-week-old transgenic mice (*right*). *C* (*I*) shows the hematoxylin/eosin staining of a section of the myocardium. *C* (*II*) shows the hematoxylin/eosin staining of the ventricles. The *left panel* shows a section from the left ventricle in the wild-type mice, and the *right panel* shows a section from the transgenic mice. *C* (*III*) shows the Masson trichrome stain from the left ventricle to demonstrate collagen deposition.

with the age-matched WT mice. The heart weight/body weight (HW/BW) ratio also increased significantly in all Tg mice during the progression to hypertrophy (Fig. 1, *A*–*B*). All four lines of mice displayed myotrophin overexpression and developed significant hypertrophy, which eventually led to heart failure. At ~36 weeks of age, the Tg mice, which overexpress cardio-specific myotrophin, developed symptoms of heart failure, including lethargy, edema, pulmonary effusion, and lack of alertness. The kidneys of the Tg mice did not differ from those of WT mice (Table I).

TABLE I

Characteristic features of Tg mice overexpressing myotrophin at 4 weeks and 9 months of age

M-mode echocardiographic data are displayed, showing several parameters in both WT and Tg mice.

	4 weeks		9 months	
	WT (n = 10)	Tg (n = 12)[a]	WT (n = 10)	Tg (n = 12)[a]
HW/BW (mg/g)	4.8 ± 0.54	5.9 ± 0.8[b]	4.7 ± 0.1	10.4 ± 0.4[b]
Kidney weight/BW (mg/g)	7.7 ± 0.1	7.6 ± 0.33	7.9 ± 0.05	7.7 ± 0.02
Myocyte cross-sectional area (μm^2)	350.2 ± 73.8	781 ± 217.3[b]	534.8 ± 109.9	2164.1 ± 693.1[b]
M-mode echocardiographic analysis				
Left atrial chamber diameter (mm)	0.16 ± 0.005	0.20 ± 0.02[b]	0.214 ± 0.022	0.285 ± 0.05[b]
Interventricular septal wall thickness (mm)	0.1002 ± 0.03	0.1140 ± 0.005[b]	0.086 ± 0.03	0.105 ± 0.004[b]
Left ventricular posterior wall thickness (mm)	0.1066 ± 0.004	0.1222 ± 0.007[b]	0.075 ± 0.016	0.09 ± 0.007[b]
Left ventricular chamber dimension (systolic; mm)	NA[c]	NA[c]	0.15 ± 0.001	0.262 ± 0.037[b]
Left ventricular chamber dimension (diastolic; mm)	NA[c]	NA[c]	0.334 ± 0.016	0.375 ± 0.01[b]
Fractional shortening (%)	50 ± 0.01	48 ± 0.03	55 ± 0.03	26 ± 0.09[b]

[a] Representing all four lines; 2–4 mice from each line.
[b] $p < 0.05$.
[c] NA, not measurable accurately.

Myotrophin Overexpression Was Associated with Histologic Lesions in Heart Tissues of Tg Mice

The LV heart walls of Tg mice (18 weeks old) were severely thickened compared with those of WT mice (Fig. 1*C* (*I–III*)) and showed concentric hypertrophy (Fig. 1*C* (*I*)). Both right and left ventricles of the Tg mice were enlarged and displayed in- creased septal thickness compared with those of the WT m- Histology examination showed typical large nuclei i- group, confirming myocyte hypertrophy (Fig. 1*C* (foci of classic myocyte disarray were observe- tissue, a change not present in the W- Fibrotic foci accompanied by dystr- observed in the Tg mice but w- (*III*)). Small foci of appar- coronary vessels.

Myotrophin Is Overex-

Myotrophin mRNA (Fig- *1* and *2*)) were increased in the - Tg lines through four generations co- mice. When re- gression analysis was done b- NA expression and HW/BW in WT and Tg mice (age- ing from 18 to 24 weeks) from all four lines, a linear correlation between myotrophin gene expression and HW/BW was observed (Fig. 2*A* (*2*); $y = 14.916x + 8.9615$ and $r^2 = 0.9691$ for Tg; $y = 15.209x - 15.744$ and $r^2 = 0.9227$ for WT). Fluorescein isothiocyanate-tagged myotrophin was abundant and distinctly visible in the myocytes from 24-week-old Tg mice from all lines, compared with age-matched WT (Fig. 2*B* (*3*)). However, myotrophin mRNA expression in the kidneys, livers, and lungs of Tg mice did not differ from that in WT mice (data not shown). As a consequence of myotrophin gene overexpression, expression of both hypertrophy marker genes (ANF and β-MHC) and proto-oncogenes (c-*fos*, c-*jun*, and c-*myc*) were also up-regulated in all four generations of the Tg mice lines (Fig. 2, *C* and *D*).

Myotrophin Overexpression Leads to Myocyte Hypertrophy in Tg Mice

To document myotrophin overexpression-induced changes in myocytes, we quantitated myocyte dimension by hematoxylin/eosin staining of heart tissue and image scanning using the Image Pro Plus software program. The cross-sectional area of myocytes in both the 4-week-old and 9-month-old mice was significantly increased (Fig. 3*A*). The myocyte cross-section increased from 350 to 781 per μm^2 ($p < 0.01$) in the 4-week-old transgenic mice. The i- s even larger in the 9-month-old mice (534–21- 0.001).

We also - hension by isolating myocytes fr- nth-old mice heart. The cr- nth-old mice was sig- + 712 per μm^2 in WT 0.001). All myocytes - s observed. These data - rtrophy was present in the - lines and four generations as - d that this hypertrophy worsened in - s (Fig. 3). The cross-sectional areas were - myocytes from each mouse (WT $n = 5$; Tg $n =$ - ting all four lines).

Cytokine and Growth Factor Gene Up-regulation Is Associated with Disease Stage in Tg Mice

We examined the relative expression of growth factors and cytokines in the Tg mice representing all four lines, using RPA (Fig. 4, $n = 5$), compared with age-matched WT mice. We studied two age groups of animals: 4-week-old mice, which represented the onset of hypertrophy, and 36-week-old mice, which represented the chronic phase of hypertrophy, during its transition to heart failure. A novel finding was the age-associated changes in expression of different cytokines. As shown in Fig. 4*A*, at 4 weeks of age, some of the cytokine transcripts were induced in Tg hearts, compared with age-matched WT. Expression of LT-β, TGF-β_2, and TGF-β_3 were significantly up-regulated in 4-week-old Tg mice compared with age-matched WT ($p < 0.05$). In the 36-week-old Tg mice, interleukin-6, macrophage migration inhibitory factor, tumor necrosis factor-α, interferon-γ, and different isoforms of the transforming growth factor-β family (TGF-β_1, -β_2, and -β_3) were significantly elevated, compared with the age-matched WT mice ($p < 0.01$). However, the percentage increase in cytokine transcripts was comparatively higher in 36-week-old Tg than in 4-week-old Tg mice. Interestingly, expression levels of interleukin-6, tumor necrosis factor-α, interferon-γ, TGF-β_2, and macrophage migration inhibitory factor did not change in the young Tg animals during initiation of hypertrophy compared with the age-matched WT mice (Fig. 4*B*). These data suggest that the cytokine-/growth factor-mediated hypertrophic process is different in young and old Tg mice, especially during transition to heart failure.

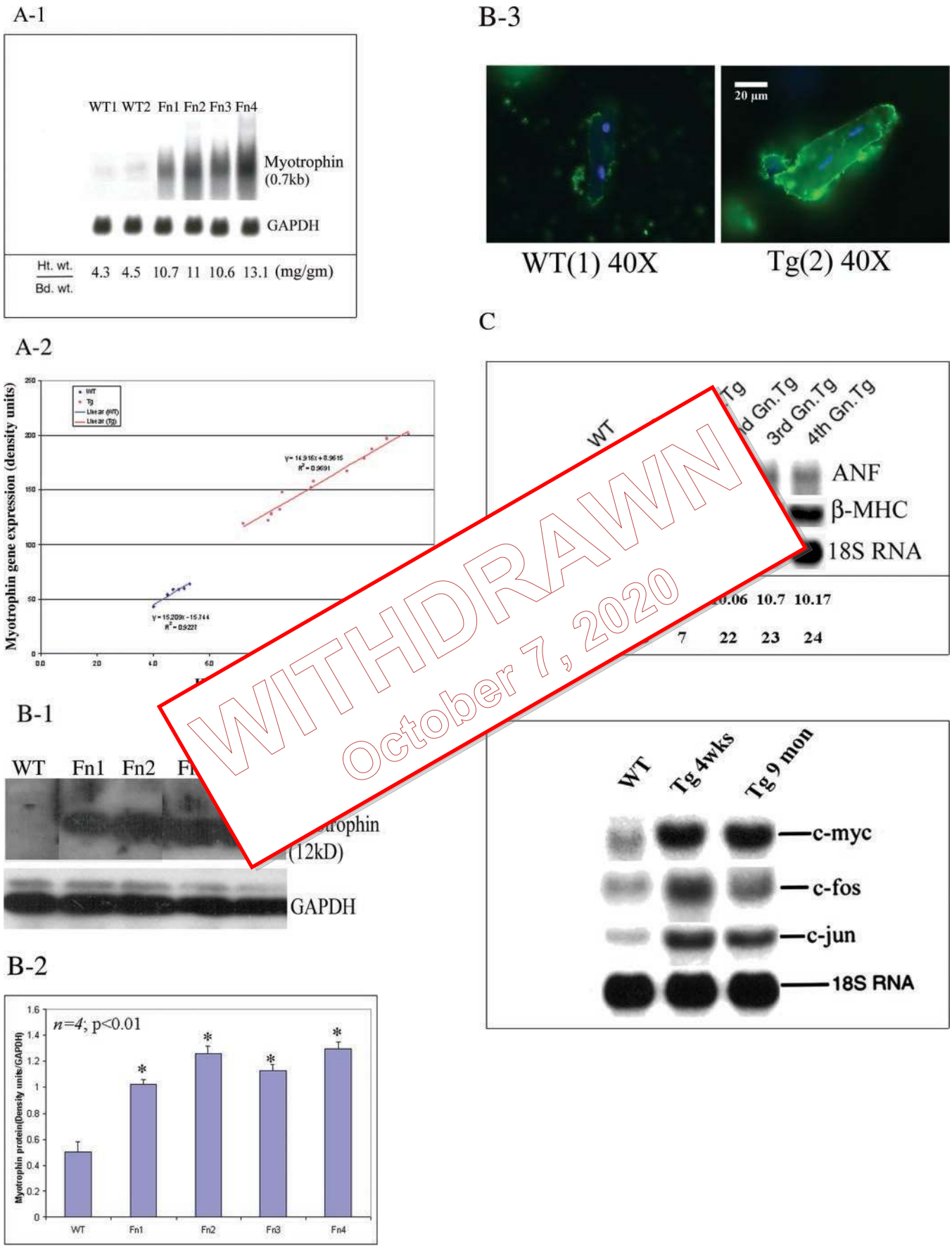

FIG. 2. *A* (*1*), Northern blot analysis of myotrophin gene expression in transgenic mice from four founders (Fn1–Fn4, 24 weeks old) compared with age-matched WT. *A* (*2*), correlation between myotrophin gene expression (*y* axis) and HW/BW in Tg and WT mice (between 16 and 24 weeks of age, representing all four lines). A significant correlation was observed between myotrophin gene expression and HW/BW (r^2 = 0.9227 for WT mice, and r^2 = 0.9691 for Tg mice). *B* (*1*), Western blot analysis showing myotrophin protein expression in 24-week-old WT and Tg mice from all four lines

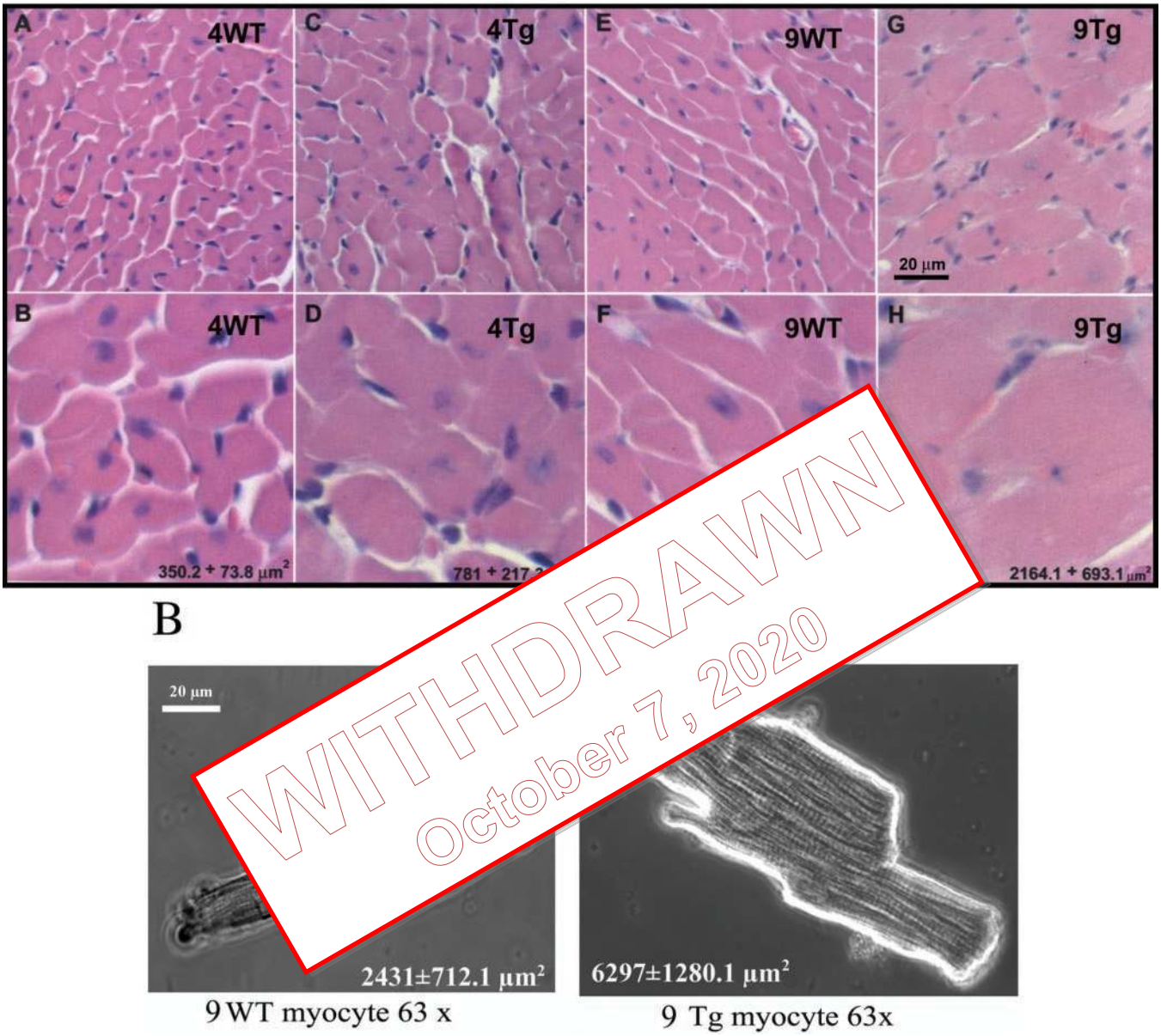

FIG. 3. *A*, quantitation of cross-sectional areas of myocytes in WT and Tg mice ($n = 5$). The *top panel* shows myocytes (stained with hematoxylin and eosin) from 4-week-old mice, WT (*extreme left*) (*A*), and Tg (*C*). *E* depicts 9-month-old WT cells, and *G* shows the myocytes from 9-month-old Tg animals at × 63 magnification. The *lower panel* represents a × 2.5 zoomed picture of the *upper panel*. *B*, myocytes from 4-week-old WT mice; *D*, myocytes from 4-week-old Tg mice; *F*, myocytes from 9-month-old WT mice; *H*, myocytes from 9-month-old Tg mice. A significant increase in the cross-sectional area was observed at as early as 4 weeks of age. This condition persisted and increased during the progression of hypertrophy (for detailed methods, see "Experimental Procedures"). This figure represents five independent experiments. *B*, myocytes isolated from 9-month-old WT (*left panel*) (× 63 magnification) and 9-month-old Tg mice overexpressing myotrophin (*right panel*) (× 63 magnification). The cross-sectional area of myocytes from Tg mice was significantly increased (2431 ± 712 μm^2 to 6297 ± 280 μm^2; $p < 0.001$) (for details, see "Experimental Procedures" and "Results"), showing significant hypertrophy in Tg mice ($n = 8$, representing all four lines).

M-mode Echocardiographic Analysis of 9-Month-old Tg Mice Revealed Progression to Heart Failure

M-mode echocardiographic data from the 4-week-old and 9-month-old Tg mice from all four lines are shown in Fig. 5 and Table I. In 4-week-old Tg mice, left atrial diameter (0.20 ± 0.02 *versus* 0.16 ± 0.005 mm), interventricular septal wall thickness (0.114 ± 0.004 *versus* 0.1002 ± 0.03 mm), and left ventricular posterior wall thickness (0.122 ± 0.007 *versus* 0.106 ± 0.004 mm) were significantly elevated, compared with their age-matched WT. Importantly, however, the functional parameter,

(Fn1–Fn4). *B* (*2*), graph showing quantification of myotrophin protein from WT and Tg mice. *B* (*3*) shows fluorescein isothiocyanate staining to localize myotrophin in 24-week-old WT and Tg (Fn2) myocytes (magnification, × 63). *C* shows increased expression of ANF and β-MHC transcripts from four generations (Gn1–Gn4), representing all four Tg lines (24 weeks old), compared with age-matched WT mice. Increased expression of ANF and β-MHC transcripts in all four generations confirmed the presence of hypertrophy in Tg mice. *D* shows increased expression of proto-oncogenes in the hearts of young and old Tg mice compared with WT mice.

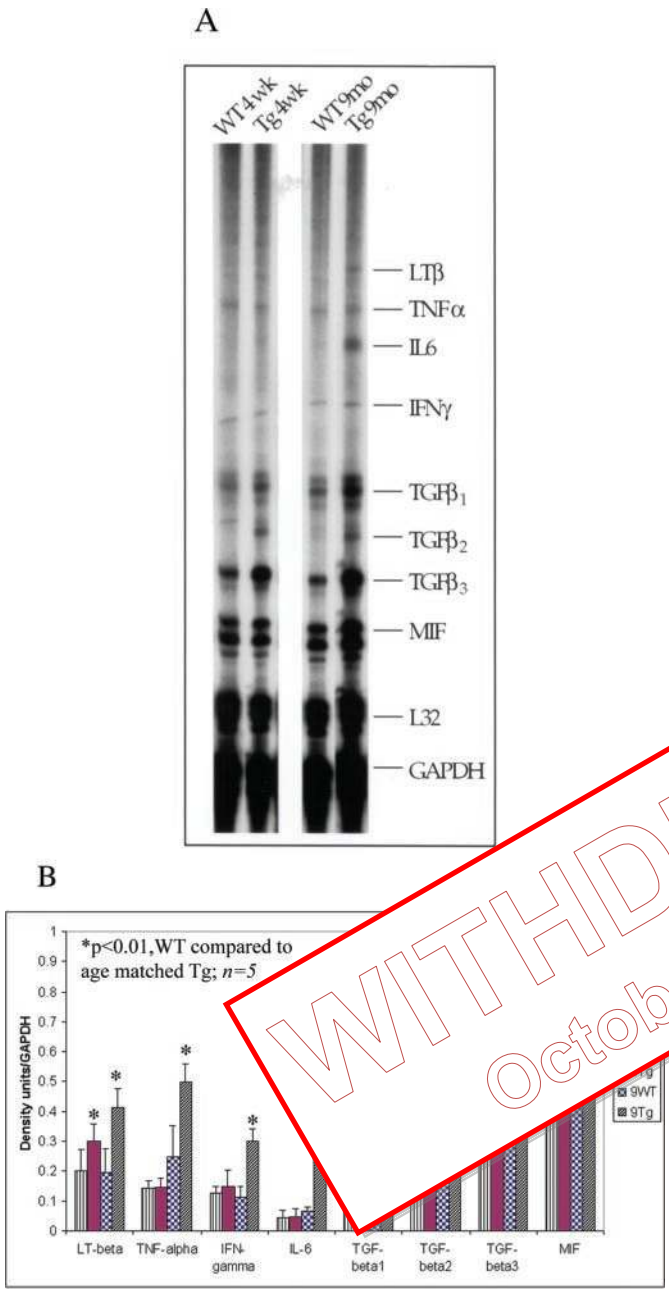

FIG. 4. *A*, a typical autoradiogram of RNase protection assays measuring cytokine expression in hearts from Tg and WT mice. Glyceraldehyde-3-phosphate dehydrogenase (*GAPDH*) was used as a loading control. An RNase protection assay was performed in five different Tg and WT mice, representing all four lines. This figure represents a typical finding from five independent experiments. *B*, estimation of the expression pattern of the cytokine transcript level normalized with glyceraldehyde-3-phosphate dehydrogenase in 4-week-old and 9-month-old WT and Tg mice hearts, representing all four lines.

fractional shortening (FS), was not changed in the 4-week-old Tg mice, compared with WT (FS = 50 ± 0.01% in WT *versus* 48 ± 0.04% in the Tg group (p = not significant)).

Echocardiographic data from 9-month-old Tg mice revealed statistically significant changes compared with the age-matched control mice: hypertrophied septum (0.105 ± 0.004 *versus* 0.086 ± 0.003 mm, $p < 0.01$), enlarged LV diastolic dimensions (0.375 ± 0.008 *versus* 0.334 ± 0.016 mm, $p < 0.01$), enlarged LV systolic dimensions (0.262 ± 0.037 *versus* 0.150 ± 0.001 mm, $p < 0.02$), and lower FS (26 ± 0.09 *versus* 55 ± 0.03% in WT, $p < 0.01$). We noted a trend toward left atrial diameter enlargement (0.285 ± 0.05 mm *versus* 0.214 ± 0.022 mm, $p < 0.01$) and increased left ventricular posterior wall thickness (0.090 ± 0.007 *versus* 0.075 ± 0.016 mm, $p < 0.05$) in the Tg mice. Furthermore, we found a large amount of pleural effusion in the Tg mice, which suggested that hypertrophy had already advanced to heart failure.

These data suggest that in the young Tg mice, cardiac function was not compromised, despite the presence of hypertrophy, whereas in the 9-month-old Tg mice, cardiac function was significantly compromised.

DNA Microarray Results

Changes in Gene Expression at the Initiation of Hypertrophy—To identify candidate genes that mediate physiological responses to myotrophin overexpression, oligonucleotide gene array analyses were performed on heart samples from Tg and age-matched WT controls. Cardiac RNAs from five transgenic and five WT animals at each age (4 weeks and 9 months) were used in the gene profiling studies. To identify genes with expression patterns that correlated with initiation of hypertrophy (4 weeks) or transition to [illegible] failure (9 months), two strategies were used. Pairwi[illegible]sons between the experimental animals of int[illegible] animal samples were used to identify [illegible] or down-regulation at a particul[illegible]ddition, SOM clustering wa[illegible]ith similar expression [illegible] of regulation within [illegible] by more than 1.8-[illegible]ed list of up-regulated [illegible]ed as Supplemental Mate-

[illegible]istently up-regulated in all pairwise [illegible]he 4-week-old Tg mice were compared [illegible]ice (9-month-old Tg and WT and 4-week-old [illegible]). When just one of the pairwise combinations was [illegible]with the others, 179 genes were induced. Of those, 39 [illegible]es were clustered in three major functional categories: extracellular matrix and cytoskeleton, cell signaling, and growth factors/transcriptional regulators. Eleven of 30 up-regulated expressed sequence tags (ESTs) had some assigned function. Among these, sarcolemmal protein SLAP, actin cross-linking protein 7, talin, glycogenin 1, and Cdc 5-like protein were elevated during the initiation of cardiac hypertrophy.

When 4-week-old Tg animals were compared with their age-matched WT animals only, a slightly different picture emerged (Table III). Seventy-four genes were up-regulated in all pairwise comparisons between 4-week-old Tg *versus* WT. These genes were clustered into six functional categories: extracellular matrix, myofibrillar and cytoskeletal protein, cellular signaling factors, growth and transcription factors, cell defense, and protein expression regulators. Forty-five known genes were down-regulated in 4-week-old Tg animals compared with the WT animals. Down-regulated genes were clustered primarily as cell signaling or mitochondrial proteins (Table III).

Changes in Gene Expression during Transition to Heart Failure—Pairwise comparisons were also used to identify genes that decreased in expression when comparing 9-month-old Tg hearts with all other samples (Table II). One hundred thirty-three genes were consistently elevated in failing hearts compared with nonfailing WT or younger Tg hearts. Fifty-one of these genes were functionally clustered into six different categories: cell signaling; growth and transcription factors; extracellular matrix and cytoskeletal protein, cell defense; apoptosis; and protein expression regulators and metabolic enzymes. Of 82 ESTs, only 11 had unknown functions.

Approximately 50 genes were down-regulated in Tg hearts compared with all other samples. Most of these genes were

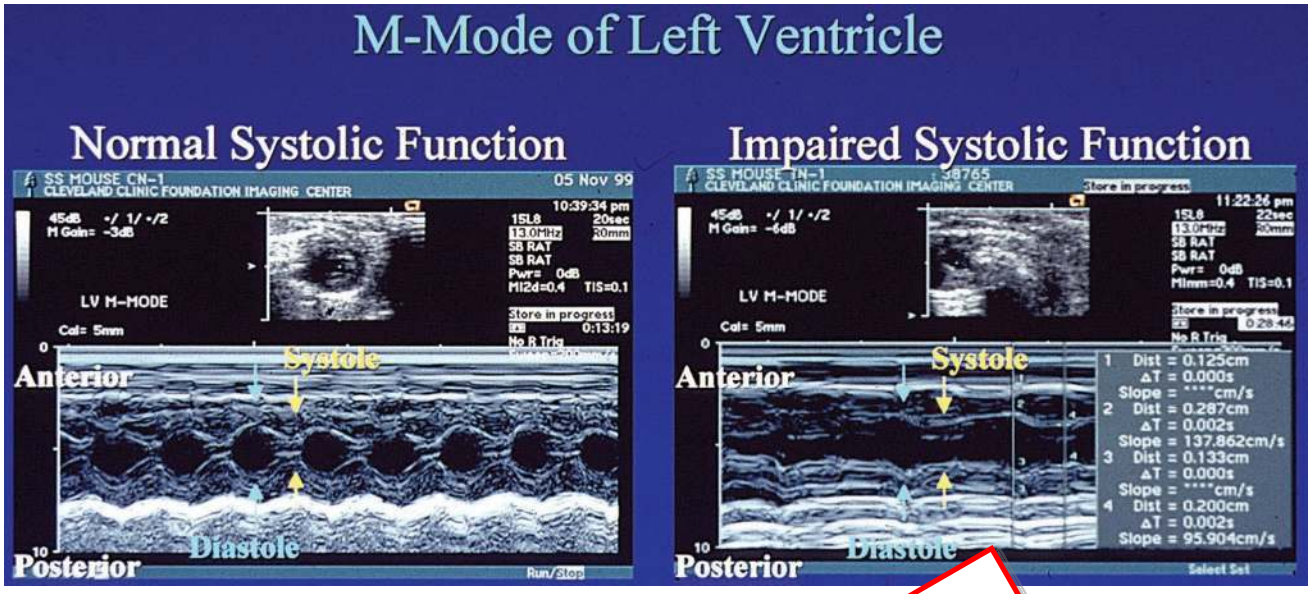

FIG. 5. **A typical M-mode echocardiogram from the 36-week-old WT and Tg mice.** Twen[illegible]ams were performed on different mice from all four lines, showing similar changes. Several echocardiogram parameters from 4[illegible]h-old mice hearts (WT and Tg) are tabulated in Table I.

identified in the aforementioned pairwise comparisons and rep[illegible]*n Heart Failure and* resented several functional groups: extracellular and cytoske[illegible] *Versus Young Tg (4* ton proteins, cellular signaling, or mitochondrial enzym[illegible] highly in 9-month-old 21 down-regulated ESTs included AP-4-related pro[illegible] genes that specifically in- H1.2, mitochondrial ribosomal protein MRPs15[illegible] weeks and 9 months, as the Tg flavoprotein, and transcription elongation [illegible] ypertrophy to heart failure. Pairwise

Pairwise comparison of 9-month-o[illegible]-old Tg and 4-week-old Tg samples iden- heart samples yielded 197 gen[illegible]hat were specifically up-regulated in Tg com- consistently up-regulated. [illegible] not in WT animals (thereby excluding age-regu- functional categories: [illegible]enes) (Table IV). Of these up-regulated genes, 44 genes cytoskeleton or protei[illegible]e classified as extracellular matrix and cytoskeleton, some genes were categ[illegible] growth and transcription factors, cell signaling factors, cell factors, cell defense prote[illegible] pro- teins involved in cell divisi[illegible] identi- fied as known ESTs among[illegible]d increased expression in failing mouse h[illegible]n to the up-regu- lated genes, 206 genes were con[illegible]down-regulated across the pairwise comparisons. For[illegible]even were clustered into functional groups, including cell signaling, matrix and cytoskeleton, or mitochondrial enzymes. Of 159 down-regulated ESTs, 16 had known functions (Table III).

Fig. 6 summarizes SOM clustering analysis of the maximally changed genes in 9-month-old Tg *versus* all as well as 4-week-old Tg *versus* all. When SOM clustering was performed using absolute gene expression values from all samples from 9-month-old Tg animals compared with either age-matched WT or 4-week-old WT or Tg mice, definitive clusters of candidate genes up- or down-regulated during the transition from hypertrophy to heart failure emerged (Fig. 6, *a* and *b*). Those maximally up-regulated include fibronectin, VCAM1, slow myosin heavy chain, matrix metalloproteinase 3, ceruloplasmin, apolipoprotein D, and MRP8. Approximately 80 genes were expressed at a higher level in three 4-week-old Tg animals when compared with all other animals (Fig. 6*c*). Included within this group were skeletal muscle actin, MLC3F, calsequestrin, immediate early genes, SLAP, glycogenin, skeletal muscle tropomyosin, talin, and disintegrin. All genes from this cluster were identified in the pairwise comparisons noted above. Interestingly, SOM analysis did not identify clusters of genes consistently down-regulated at this early developmental time point (data not shown).

Similar pairwise comparisons identified 30 cardiac genes down-regulated in 9-month-old Tg animals compared with 4-week-old Tg animals. These genes clustered into several functional groups: extracellular matrix and cytoskeleton proteins, mitochondrial enzymes, cell signaling factors, or cell cycle regulators. Fifteen known ESTs in this group included cyclophilin D, tropomyosin 5, exportin 1, and Ras-related protein RAL1.

DISCUSSION

This study reinforces the proofs we have previously presented that myotrophin is a significant causal factor in the hypertrophy/heart failure continuum. Data presented here document the effects of myotrophin protein overexpression at molecular, cellular, morphological, and functional levels in a specially developed line of Tg mice. These data indicate that myotrophin overexpression initiates cardiac hypertrophy, eventually progressing to heart failure, a process associated with changes in expression of proto-oncogenes, ANF, β-MHC, and cytokines. Importantly, using this model and the new tools of state-of-the-art DNA microarray analysis (Fig. 6 and Tables II and III), we have elucidated patterns of gene up-regulation and down-regulation that may be involved during initiation of cardiac hypertrophy and progression to heart failure in humans.

TABLE II

Changes in gene expression at the initiation of hypertrophy (Tg 4-week-old (4 Tg) versus all) and during transition to heart failure (Tg 9-month-old (9 Tg) versus all) (n = 5)

Accession no.	9 Tg *versus* all	Accession no.	4 Tg *versus* all (up-regulated genes)
Up-regulated genes		Extracellular matrix and cytoskeletal proteins	
Cell signaling		M12347	Skeletal muscle α-actin
D16497	Natriuretic peptide precursor B	X12973	MLC3F gene for myosin alkali light chain
K02781	Natriuretic peptide precursor A	U93291	Skeletal muscle calsequestrin
M84487	Vascular cell adhesion molecule 1	M81086	Skeletal muscle β-tropomyosin
Extracellular matrix and cytoskeletal proteins		X66405	Procollagen type VI α1
X58251	Procollagen type 1α2	Cell signaling	
M18194	Fibronectin	L47650	Signal transducer and activator of transcription 6
AJ223362	Slow myosin heavy chain β	U43187	MEK kinase 3
X66402	Matrix metalloproteinase3	L78075	Cdc 42 (Rho family of GTPase)
Inflammation and cell defense		Growth factor and transcription factor	
M33960	Plasminogen activator inhibitor-1	X61940	Growth factor-inducible early response gene
U49430	Ceruloplasmin	M57647	Mouse mast cells growth factor
AF022110	Tumor necrosis factor family	X72310	Tran[illegible]ption factor DP1
Protein expression		AF035717	T[illegible]tion factor 21(Pod1)
M70642	Fibroblast inducing secreted protein	ESTs	
X82648	Apolipoprotein D	AW124175	[illegible]ssociated protein (SLAP)
M83218	Calcium binding protein, MRP-8	AI843799	[illegible]ing protein 7
Z11911	Glucose-6-phosphate dehydrogenase	AW12[illegible]	[illegible]port inner membrane
Growth factor and transcription factor			
M32745	Transforming growth factor-β[illegible]		[illegible]III
X81581	Insulin-like growth factor		
M61007	CCAAT/enhancer bin[illegible]		[illegible]rotein
Apoptosis			[illegible]se-promoting complex subunit 4
AB019600	Caspase-9		[illegible]integrin and metalloprotease domain 19
AF041054	Nip3		Mouse Ras-related protein RAL-A
ESTs			
AW122039			
AA981257			
AI848508			
Down-regulated genes			
Extracellular matrix a[illegible] cytoskeletal proteins			
U09181			
X12972	[illegible]yosin alkali [illegible]entricular slow		
Metabolism and mitochondrial enzymes			
X53157	Mitochondrial cytochrome c oxidase		
AF058955	ATP-specific succinyl CoA synthetase β		
X51905	Lactate dehydrogenase		
Cell signaling			
M28723	Antioxidant protein 1		
U70068	Potassium voltage-gated channel, subfamily Q		
ESTS			
AI526902	Cytochrome *c* reductase		
AI836029	Mitochondrial ribosomal protein MRPs15		
AI849767	ATP synthase		
AI851178	Electron transfer flavoprotein		
AI132239	Tcea3 transcription elongation factor A protein		

We documented several novel mechanistic changes that occur during the transition from hypertrophy to heart failure. We confirmed that myotrophin overexpression resulted from increased myotrophin mRNA and protein levels in all lines and generations of Tg mice (Fig. 2). Importantly, the increase in myotrophin triggered a significant increase in cytokines and growth factors such as LT-β, tumor necrosis factor-α, interferon-γ, interleukin-6, TGF-β_1, TGF-β_2, TGF-β_3, and macrophage migration inhibitory factor, in 9-month-old Tg mice, when chronic hypertrophy advanced to heart failure (Fig. 4), whereas, at 4 weeks of age, three genes (LT-β, TGF-β_2, and TGF-β_3) were up-regulated in Tg mice, compared with the age-matched WT. Echocardiographic data showed significant hypertrophy of left ventricle and septum (asymmetric hyper-

TABLE III

Changes in gene expression at the initiation of hypertrophy (4-week-old Tg (4 Tg) versus 4 WT) and during transition to heart failure (9-month-old Tg (9 Tg) versus 9 WT)

Accession no.	9 Tg versus 9 WT (n = 5)	Mean -fold change	Accession no.	4 Tg *versus* 4 WT (n = 5)	Mean -fold change
Up-regulated genes			Up-regulated genes		
Cell signaling			Extracellular matrix and cytoskeletal proteins		
D16497	Natriuretic peptide precursor B	2.3	X12973	MLC3F gene for myosin alkali light chain	2.0
K02781	Natriuretic peptide precursor A	5.1	U93291	Skeletal muscle calsequestrin	1.8
M84487	Vascular cell adhesion molecule 1	3.1	U03419	Procollagen α 1 type 1	2.5
X66449	Calcyclin	2.7	X66976	Collagen 8a1	2.3
Z68618	Transgelin	3.2	X13986	Minopontin	12.3
U07982	Endothelin 1	2.3	M28729	Tubulin α 1	1.8
Extracellular matrix and cytoskeletal proteins			Cell signaling		
X13986	Minopontin	70.0	AF020185	Protein inhibitor of nitric-oxide synthase	2.3
X58251	Procollagen type 1 alpha 2	3.1	D16497	Natriuretic peptide precursor type B	2.4
M18194	Fibronectin	3.5	M84487	VCAM 1	2.3
X70854	Fibulin	2.6	X77952	Endoglin	1.9
AJ223362	Slow myosin heavy chain β	3.1	M69260	Lipocortrin 1	1.9
X66402	Matrix metalloproteinase3	4.1	Cell defense		
Protein expression			X15591	Cytot[illegible]yte-associated protein 2 α	3.9
X82648	Apolipoprotein D	7.3	U69491	I[illegible]r	1.5
M83218	Calcium binding protein,MRP-8	8.1	J03520	[illegible]ivator	1.6
Z11911	Glucose-6-phosphate dehydrogenase	6.2	M19681	[illegible]2	4.1
Growth factors and transcription factors			U49430		2.5
X81581	Insulin-like growth factor protein	8.9	Gr[illegible]		
M61007	CCAAT/enhancer-binding protein	2.1		[illegible]r β	2.8
M32745	Transforming growth factor- [beta-3			[illegible]or 21	1.8
Apoptosis and cell division				[illegible] containing gene 2	5.9
AB019600	Caspase-9				
AF041054	Nip3			Calmodulin	1.8
X59846	GA[illegible]			Fibroblast-inducible secreted protein	4.2
AF005886				Calpactin 1 light chain	2.1
Cell defense				Cysteine-rich glycoprotein SPARC	2.3
AF022110			[illegible]ted genes		
M33960	Pl[illegible] in[illegible]		[illegible]xtracellular matrix and cytoskeletal proteins		
U49430	Ceru[illegible]		M12481	Cytoplasmic β actin	0.6
V00835	Metall[illegible]	3.2	U09181	Cardiac troponin I	0.8
ESTs			AF093624	Nspl1	0.6
AF025821	AHSG, ty[illegible] inhibitor	5.2	Cell signaling		
AA688938	BclXl	1.9	U94423	Mouse MEF2A mRNA	0.4
AW125874	Cdk3	2.4	L20343	Calcium channel β 2	0.6
AI843106	p53 homologue	3.1	M31131	Cadherin 2	0.6
AI849615	Gas 5	2.4	M63801	Connexin 43	0.4
AW124175	Sarcolemma- associated protein	1.5	U83509	Angiopoietin 1 mRNA	0.5
Down-regulated genes			AF020737	Fibroblast growth factor 13	0.4
Extracellular matrix and cytoskeletal proteins			AF080580	CLK-1 mRNA	0.8
U09181	Cardiac troponin I	0.43	AF029982	SERCA 2	0.6
M91602	Myosin light chain 2	0.6	Mitochondrial enzymes		
M29793	Slow cardiac troponin C	0.6	Z49204	Nicotinamide nucleotide transhydrogenase	0.7
Mitochondrial enzymes			Z11774	Fumarylacetoacetate hydrolase	0.6
X53157	Mitochondrial cytochrome c oxidase	0.6	U12961	NAD(P)H oxidoreductase 1	0.7
AF058955	ATP-specific succinyl-CoA synthetase β	0.6	M76727	Pyruvate dehydrogenase E1 α subunit	0.6
Cell signaling			Protein expression		
M28723	Antioxidant protein 1	0.7	X17069	Transition protein TP2	0.7
AF029982	SERCA 2	0.6	X16493	Zinc finger protein 1	0.7
U06924	STAT1	0.7	AF107780	Potassium channel Kv4.2 mRNA	0.3
ESTs					
AA870675	ATP synthase	0.58			
AW123564	Global ischemia- induced protein	0.4			
AI836740	Aconitase 2	0.6			
AI852862	Fumerate hydratase	0.5			
AI181132	Creatine kinase	0.5			

TABLE IV
Comparison of gene expression between heart failure and initiation of hypertrophy: Tg (9 months old) versus Tg (4 weeks old) (n = 5)

Accession no.	Gene description	Mean -fold change
Up-regulated genes		
Extracellular matrix and cytoskeletal proteins		
AF061272	C-type lectin	20.3
M18194	Fibronectin mRNA	2.5
X66402	Matrix metalloproteinase 3	4.1
AB007848	Bone matrix protein osteomodulin	2.7
U04541	α-Tropomyosin, slow	2.5
X67348	Procollagen type X, α	2.3
Growth and transcription factors		
X81580	Insulin-like growth factor-binding protein 2	2.7
U17291	Transcription factor AP2	3.1
Cell signaling		
U12884	Vascular cell adhesion molecule 1	2.9
U59758	p53 variant mRNA	1.8
U28423	Protein kinase inhibitor p58	4.6
M21856	Cytochrome P450	1.6
U40930	Oxidative stress-induced protein	2.6
AF047838	Calcium-sensitive chloride conductance protein 1	4.4
Cell defense		
AF019048	Tumor necrosis factor superfamily member	3.1
M33960	Plasminogen activator inhibitor (PAI-1)	6.4
M17015	Lymphotoxin A	
Protein expression		
M83219	Intracellular calcium-binding	1.8
U08373	Calmegin (Ca^{2+}-binding	2.3
M70642	Fibroblast-inducible	1.8
Apoptosis		
AF041054	Nip3 (Bcl2-bi	2.4
AB019600	Caspase	1.9
ESTs		
AI842277		3.1
AI846289		2.2
AI505453		2.1
AA612146		2.3
Down-regulated genes		
Cytoskeletal proteins		
M12347		0.4
M21495		0.5
M18775	protein Tau	0.5
Mitochondrial enzy		
U77128	ATP synthase coupling factor 6	0.6
M76727	ehydrogenase E1 α	0.7
U59282	nthase E subunit	0.5
X53157	tochrome *c* oxidase	0.7
AB021122	TIM 23	0.55
Cell signaling		
M63801	Connexin 43	0.3
U97170	Protein kinase C inhibitor γ	0.6
L02526	Mitogen-activated protein kinase kinase	0.7
AF020185	Protein inhibitor of nitric-oxide synthase	0.3
X53584	HSP60	0.4
X53476	HMG 14	0.6
L78075	Cell division cycle 42	0.6
ESTs		
AW122022	Cyclophilin D	0.5
AW124594	Mitochondrial import inner membrane translocase	0.5
AI848416	Mitochondrial ribosomal protein L36	0.4
AI835847	NAPD:ubiquinin oxidoreductase	0.6
AI849767	H^+-transporting ATP synthase	0.6
AW125336	Pyruvate dehydrogenase β	0.5

trophy) in 36-week-old Tg mice hearts, a typical change observed in human hypertrophy. Mice afflicted with hypertrophy also had severely compromised cardiac function associated with pleural effusion, a common occurrence during human heart failure. However, this compromised function did not occur in the hypertrophied hearts of young 4-week-old Tg mice despite presence of hypertrophy. Our data also suggest that atrial enlargement arises from mitral and tricuspid valve regurgitation, which occurs because the ventricular cavity enlarges, causing an incomplete sealing in these valves. This cluster of symptoms mimics human cardiomyopathic hypertrophy with end-stage heart failure. Although other Tg models have been reported (14, 15), none have studied the progression of hypertrophy that advances to heart failure in the manner we have described. Previously, using isolated myocytes, we have shown that the mode of action of myotrophin protein is mediated through protein kinase C and NF-κB signaling pathways (16). This *in vivo* model, overexpressing myotrophin, provided us with the opportunity to dissect out the role of myotrophin-induced signaling pathways for the initiation process of cardiac hypertrophy and its progression to heart failure. Work is in progress to determine protein kinase C and NF-κB cascade in Tg hearts at 4 weeks, 16 weeks, and 9 months compared with their age-matched WT.

This model provided the opportunity to further the genome-wide screening of cardiac tissue as a tool to identify new genes

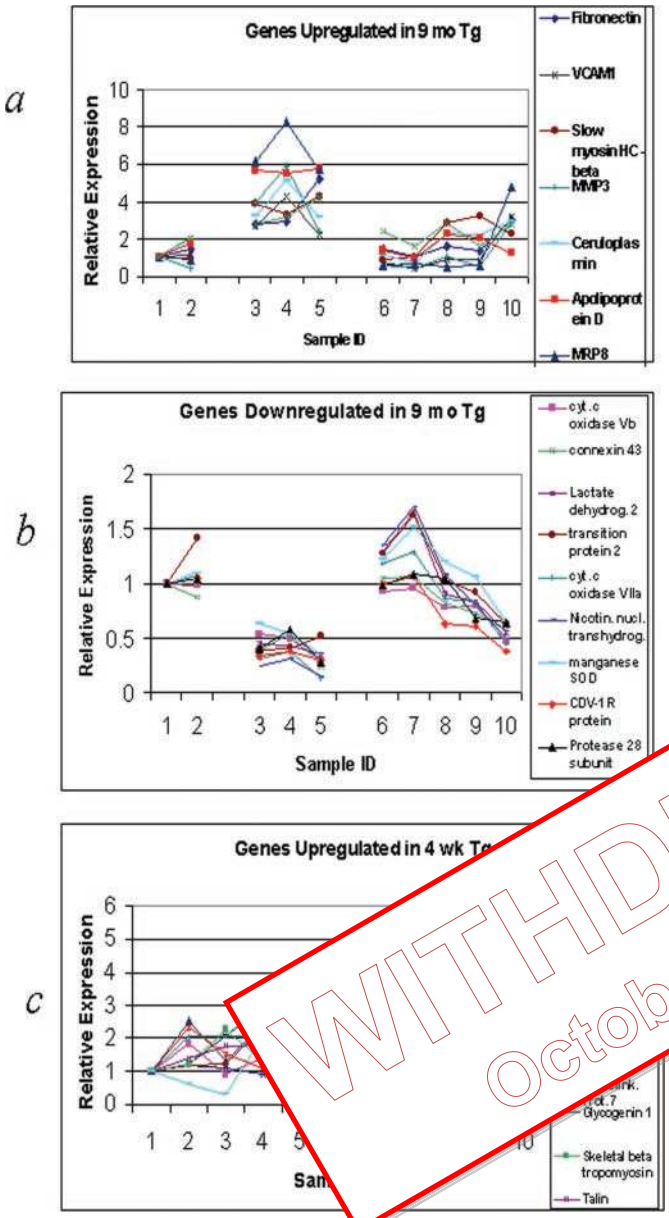

FIG. 6. **Gene expression patterns in WT and Tg animals.** SOM cluster analysis was used to identify gene clusters that exhibited similar expression patterns. Affymetrix signal values from genes representing three of the identified expression patterns were normalized to sample 1 (a 9-month-old WT animal), and the relative expression values were plotted for each animal. The sample ID numbers represent the 9-month-old WT animals (*1* and *2*), 9-month-old Tg mice (*3–5*), 4-week-old WT mice (*6* and *7*), and 4-week-old Tg mice (*8–10*). An abbreviated gene name is provided for each gene assessed.

altered during initiation, progression, and transition from hypertrophy to heart failure. This study is unique because this type of experiment is not possible in humans. The alteration of several hypertrophy-associated genes reported in recent gene array studies in human failing heart (17) were found to be similar to the murine heart failure model overexpressing myotrophin, reported in this study. For the first time, we documented the alterations of gene clusters that participate during the initiation of hypertrophy and during the transition from hypertrophy to heart failure (Table II). Our data also suggest that the initiation of hypertrophy utilizes a transcriptional program involving specific sets of genes, which are distinct from those that operate during the transition phase. Characterization of the expression of these novel genes during initiation and transition phases could provide new insights into cardiac remodeling.

In failing hearts, natriuretic peptide precursors type A and B were ranked as the top candidate genes when compared with either age-matched WT or with the total of all young WT and Tg samples. SOM clustering analysis identified the maximally changed gene expressions during both initiation and progression of hypertrophic process. The functions of many of them are yet to be defined during hypertrophy to heart failure. This gene cluster continues to be expressed during the progressive deterioration of cardiac function (18). In addition, significantly increased expression of extracellular matrix proteins, like collagen type I and type VIII, fibronectin, C-type lectin, and matrix metalloproteinases, was observed in failing hearts (19). Growth factors like TGF-β_2, TGF-β_3, tumor necrosis factor-α, insulin-like growth factor, and hypoxia-inducing factor 1α can be important during the transition from hypertrophy to heart failure. Genes involved in fatty acid metabolism (*e.g.* apolipoprotein-D and -E) and glucose metabolisms (glucose-6-phosphate dehydrogenase) were up-regulated, whereas lactate dehydrogenase and fatty [illegible]inding proteins were down-regulated. Several m[illegible] enzymes were consistently and significantly [illegible]n failing hearts compared with either [illegible]earts, a finding that may explain [illegible]roduction during heart fail[illegible] such as CIDE-A, Bcl2-[illegible]iling hearts signifies [illegible]onein 1 and 2 are [illegible]ns whose antioxidant [illegible]s in the heart were reported [illegible]*et al.* (17), we found increased [illegible]ein proteins as well as such other cell [illegible]GAS 6, cyclin 1, and histone H1. This [illegible]ancy indicates that cell death and cell regen-[illegible]occur simultaneously in the failing heart. No such [illegible]were found when 36-week-old Tg mice were compared [illegible]ch 4-week-old Tg mice, although NIP3 and caspase-9 were up-regulated in old Tg animals. Apoptosis was not evident during the initiation phase of hypertrophy, yet induction of cyclin and *cdk* genes started as early as 4 weeks of age in Tg mice hearts.[2]

Our data showed that initiation of hypertrophy was associated with induction of fewer genes. Compared with genes from failing hearts, interestingly, no genes were down-regulated during the initiation of hypertrophy (4-week-old Tg mice). Among the cytoskeletal proteins, myosin alkali light chain, skeletal muscle calsequestrin, β-tropomyosin, and transcriptional activators like mitogen-activated protein kinase/extracellular signal-regulated kinase kinase kinase 3, STAT6, Pod1, and DP1 were up-regulated in the hearts of 4-week-old Tg mice. Combining all of these findings, the data are expected to provide information for changes in cardiac metabolism during onset of hypertrophy and its transition to heart failure.

In conclusion, this new Tg mouse model of hypertrophy resulting from myotrophin overexpression, leading to heart failure, is important because of its similarity to end-stage heart failure in human beings in both molecular (gene expression of hypertrophy marker genes, proto-oncogenes, cytokines, and growth factors) and physiological parameters (pleural effusion and lethargy). Heart failure occurred in all of our Tg mice sacrificed to date (n = 150), and the average life span was 8–11 months in the F_1, F_2, F_3, and F_4 generations. Several growth factors and cytokines were increased during the initiation

[2] S. Sarkar, M. Chawla-Sarkar, D. Young, K. Nishiyama, M. E. Rayborn, J. G. Hollyfield, and S. Sen, manuscript under preparation.

phase and during the transition of hypertrophy to heart failure. Comparison of the gene array data between the initiation of hypertrophy and its transition to heart failure involves differential activation of functional gene clusters. Up-regulation of growth factors, calcium-binding proteins, proteins regulating programmed cell death, and extracellular/cytoskeletal proteins as well as down-regulation of mitochondrial proteins and cytoskeletal/myofibrillar proteins mark the transition phase, which is associated with severely compromised heart function, thereby differing from the mechanisms of the initiation process of hypertrophy as well as those operating in nonfailing WT hearts.

The intricate, multifaceted process of heart failure, especially its transition from longstanding hypertrophy to heart failure, involves many factors. Eventual heart failure is probably the result of cross-talk between neurohumoral mechanisms and growth factors. Our new genetic data, added to our prior findings based on molecular and biochemical data, convincingly demonstrate that myotrophin is a factor that not only initiates hypertrophy but is also associated with the progression to heart failure. We expect that this new mouse model will provide the key to elucidate further molecular mechanisms that occur during advancement of hypertrophy to heart failure and will facilitate the design of effective therapies.

Acknowledgments—The gene array studies were conducted in the University of Toledo Center for Molecular Biology. We thank Dr. Jef… Robbins of University of Cincinnati for α-MHC promoter, Dr. M… Chawla-Sarkar of the Taussig Cancer Center for assistance… RPA, Christine Kassuba for editorial assistance, and JoAnne Holl for expert secretarial support.

REFERENCES

1. Chien, K. R., Zhu, H., Knowlton, K. U., Miller-Hance, W., van-Bilsen, W., O'Brien, T. X., and Evans, S. M. (1993) *Annu. Rev. Physiol.* **55,** 77–95
2. Sadoshima, J., and Izumo, S. (1997) *Annu. Rev. Physiol.* **59,** 551–571
3. Sen, S., Tarazi, R. C., Khairallah, P. A., and Bumpus, F. M. (1974) *Circ. Res.* **35,** 775–781
4. Sen, S. (1987) *Circulation* **75,** I81–I84
5. Sen, S., Kundu, G., Mekhail, N., Castel, J., Misono, K., and Healy, B. (1990) *J. Biol. Chem.* **265,** 16635–16643
6. Mitra, S., Timor, A., Gupta, S., Wang, Q., and Sen, S. (2001) *Cytogenet. Cell Genet.* **93,** 151–152
7. Mukherjee, D. P., McTiernan, C. F., and Sen, S. (1993) *Hypertension* **21,** 142–148
8. Sil, P., Mukherjee, D. P., and Sen, S. (1995) *Circ. Res.* **76,** 1020–1027
9. Sivasubramanian, N., Adhikary, G., Sil, P. C., and Sen, S. (1996) *J. Biol. Chem.* **271,** 2812–2816
10. Iwaki, K., Sukhatme, V. P., Shubeita, H. E., and Chien, K. R. (1990) *J. Biol. Chem.* **265,** 13809–13817
11. Sil, P., Kandaswamy, V., and Sen, S. (1998) *Circ. Res.* **82,** 1173–1188
12. Bialkowska, K., Kulkarni, S., Du, X., Goll, D. E., Saido, T. C., and Fox, J. E. (2000) *J. Cell Biol.* **151,** 685–696
13. Tamayo, P., Slonim, D., Mesirov, J., Zhu, Q., Kitareewan, S., Dmitrovsky, E., Lander, E. S., and Golub, T. R. (1999) *Proc. Natl. Acad. Sci. U. S. A.* **96,** 2907–2912
14. Vikstrom, K. L., Bohlmeyer, T., F… r, S. M., and Leinwand, L. A. (1998) *Circ. Res.* **82,** 773–778
15. James, J. F., Hewett, T… s, J. (1998) *Circ. Res.* **82,** 407–415
16. Gupta, S., Purcell… Sen, S. (2002) *J. Cell Biol.* **159,** 1019–1028
17. Tan, F. L… n-Hansen, C., McCarthy, P. M., You… *Natl. Acad. Sci. U. S. A.* **99,**
18. …to, S., Hata, T., and Yanaga,
…me, H., Speiser, B., Friedl,
…14
…**22,** 263–273